Physicochem. Probl. Miner. Process., 62(6), 2026, 242385

http://www.journalssystem.com/ppmp

Physicochemical Problems of Mineral Processing

ISSN 1643-1049
© Wroclaw University of Science and Technology

Study on the selective adsorption mechanism of guar gum in the flotation separation of diaspore and kaolinite

Yongshuai Fu [1], Jiacheng Li [1], Zelin Du [1], Jin Yao [2], Xiufeng Gong [2], Jianwei Yu [2]

[1] School of Mining Engineering, Heilongjiang University of Science and Technology, Haerbin 150020, Heilongjiang, China

[2] School of Resources and Civil Engineering, Northeastern University, Shenyang 110819, Liaoning, China

Corresponding author: G15524147233@163.com (Xiufeng Gong)

Abstract: This study investigated the selective adsorption mechanism of guar gum (GG), a green and efficient regulator, in the flotation separation of diaspore and kaolinite. Under a sodium dodecyl sulfonate (SDS) system, flotation tests showed that GG achieved a maximum flotation difference of 72.99% between the two minerals, along with an Al_2O_3/SiO_2 ratio of 9.47 and a selectivity separation index of 5.01. Contact angle measurements revealed that GG slightly reduced the contact angle of diaspore (by 3.56°) but significantly reduced that of kaolinite (by 14.51°), thereby enhancing the floatability contrast between them. Zeta potential tests confirmed strong GG adsorption on kaolinite and weak adsorption on diaspore, as the shift in kaolinite's isoelectric point after GG treatment was more pronounced than that of diaspore. Fourier transform infrared spectroscopy indicated that the strong adsorption of GG on kaolinite hindered subsequent SDS adsorption, whereas on diaspore, GG adsorbed weakly, allowing SDS to still adsorb effectively. XPS analysis further showed that GG had only minor effects on the Al peak shifts and Al content changes of both minerals, but significantly affected the Si peak shift and Si content on kaolinite surfaces, reflecting selective adsorption of GG onto kaolinite and specifically onto its Si sites. Consequently, during flotation, kaolinite is inhibited and sinks, while diaspore remains floating, enabling efficient separation of the two minerals.

Keywords: kaolinite, flotation, selective adsorption, diaspore, guar gum

1. Introduction

Aluminum is the second most widely used metal globally, after steel (Yu et al., 2025). Owing to its low specific gravity, excellent electrical and thermal conductivity, high formability, and a range of other advantageous physical and mechanical properties, aluminum is extensively employed across diverse sectors of the national economy (Zhao et al., 2025; Xu et al., 2026). Currently, the construction, transportation, and packaging industries collectively account for more than 60% of global aluminum consumption (Zhang et al., 2022; Gong et al., 2024a; Xie et al., 2025). In addition, aluminum serves as a critical raw material in the electrical, aerospace, machinery, and consumer appliance industries (Szerenyi et al., 2025; Yu et al., 2024).

China's bauxite resources are predominantly of the diaspore type, characterized by high alumina content, high silica content, low iron content, geographically concentrated distribution, and relatively high processing complexity (Xia et al., 2009). Diaspore-type bauxite consists primarily of diaspore and kaolinite, with iron-bearing minerals as secondary constituents (Jiang et al., 2014). Based on ore texture and structure, it is classified into four main types: soil-like, bean-like, detrital, and dense, among these, soil-like bauxite exhibits the highest quality and most favorable metallurgical properties (Liu et al., 2011; Hassan et al., 2025).

In order to better remove gangue minerals from diaspore resources, some scholars have carried out theoretical research on flotation and achieved certain separation results. Li et al. (2021) introduced D-phenylalanine (D-phe) into the sodium oleate (NaOl) flotation system, which increased the flotation recovery of diaspore from 77.13% to 91.07%, and the recovery of kaolinite from 16.27% to 13.75%, which improved the collection and selectivity of diaspore. Zhang et al. (2-19) investigated the effect of sulfuric acid pretreatment on the flotation separation of monazite and kaolinite using X-ray photoelectron

DOI: 10.37190/ppmp/242385

spectroscopy. The results showed that the Al/Si atomic ratio on the surface of kaolinite decreased after acid treatment, and the adsorption capacity for dodecylamine hydrochloride was enhanced, promoting effective separation between kaolinite and monazite. In order to improve the flotation recovery rate of fine-grained kaolinte, Ouyang et al. (2024) synthesized a new type of tetradecylamine propoyloxime (TPA) collector. Compared with the traditional collector tetradecylamine (TDA), the TPA system has better flotation performance for fine-grained kaolinte, with a micro flotation test recovery rate of 90.5%. Chang et al. (2021) used experiments and molecular dynamics simulation methods to comprehensively study the impact of polyacrylamide (PAM) on bauxite flotation, and concluded that after the concentration of PAM exceeds the critical value, the recovery rate and selectivity of bauxite flotation are rapid, and high concentration of PAM may hinder the adsorption of collectors through steric hindrance.

Guar gum is a plant gum made from the endosperm of the leguminous plant guar bean seeds after peeling and removing the embryo (2007). It is then subjected to pressure hydrolysis, 20% ethanol precipitation, centrifugal separation, drying, and crushing. It is mainly produced in dry areas of Pakistan, India, and the southeastern United States (Gong et al., 2023a; Wang et al., 2005; Ding et al., 2026). The GG used in this study has the molecular formula $C_{10}H_{14}N_5Na_2O_{12}P_3$ and a molecular weight of 535.15. Due to its structure similar to cellulose, guar gum can quickly adsorb on the surface of fibers and provide a large number of hydroxyl groups for the formation of hydrogen bonds between fibers, effectively promoting the bonding between fibers (Rath et al., 2000). In addition, the abundant phosphate and hydroxide groups present in guar gum molecules are prone to interact with metal ions on mineral surfaces (Vidal et al., 2015).

In order to enrich the flotation separation practice of diaspore and kaolinite, sodium dodecyl sulfonate as collector and guar gum as regulator were selected in this study. With the help of modern surface analysis methods, the adsorption mechanism of flotation reagent on the surface of two minerals was analyzed, aiming to lay a theoretical foundation for the flotation purification of diaspore-type bauxite.

2. Experimental

2.1. Minerals and reagents

Referring to our previous preparation method (Yu et al., 2025), the products with a particle size of −0.074 +0.045 mm and a particle size of less than 5 μm in kaolinite and diaspore samples are selected for flotation feeding and detection analysis respectively (Gong et al., 2023b). The particle size and composition results of the samples are shown in the figure below.

As shown in Fig. 1, the volume-weighted mean particle sizes (D [4,3]) were 57.66 μm and 55.14 μm for diaspore and kaolinite, respectively, with both exhibiting relatively uniform particle size distributions—favorable conditions for flotation tests. The theoretical contents of Al_2O_3 in kaolinite and diaspore are 39.50 % and 84.98 %, respectively. As shown in Fig. 2, the Al_2O_3 content of the kaolinite and diaspore samples were 37.70 % and 77.44 %, respectively. In this study, the ratio of the tested content of the characteristic elements (i.e., Al_2O_3 in kaolinite and diaspore) to their theoretical content was taken as the purity of kaolinite and diaspore, which were 95.44 % and 91.13 %, respectively, in accordance with the requirements of flotation tests (Yang and He, 2025).

The collector, sodium dodecyl sulfonate (SDS, analytical grade, >98%), was purchased from Sinopharm Chemical Reagent Co., Ltd., while the inhibitor, guar gum (GG, analytical grade, 99%, viscosity 5000-5500 cps), was obtained from Tianjin Comeo Chemical Reagent Co., Ltd. The pH regulators HCl (chemically pure, 37%) and NaOH (chemically pure, 99%) were supplied by Shanghai Ding Biochemical Technology Co., Ltd.

The relative content characteristics of each component element in guar gum were obtained through X-ray photoelectron spectroscopy analysis in the experiment, and the test results are shown in Table 1. It shows that among the main components of guar gum, the contents of C 1s, O 1s, N 1s, and P 2p account for 73.23%, 23.74%, 2.31%, and 0.72%, respectively.

Table 1. Relative atomic content of main elements of guar gum

Element	C 1s	O 1s	N 1s	P 2p
Atomic (%)	73.23	23.74	2.31	0.72

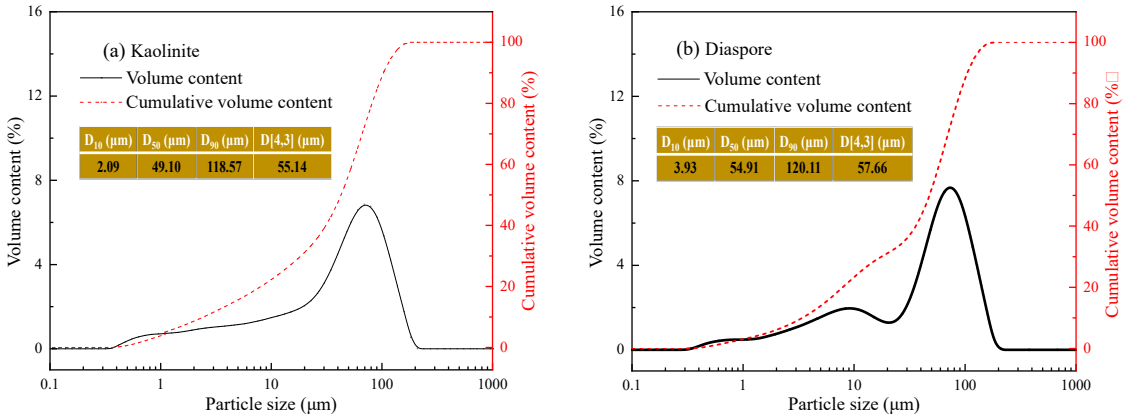


Fig. 1. Particle size distribution of kaolinite and diaspore (−0.074 +0.045 mm)

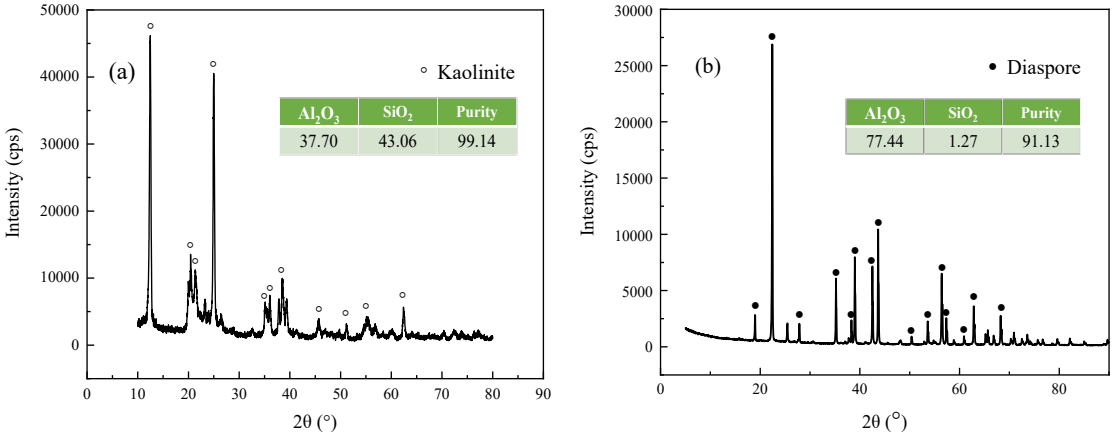


Fig. 2. X-ray diffraction patterns of kaolinite and diaspore

2.2. Method

The micro flotation experiment used an XFG-II hanging tank flotation machine with a speed of 1602 r/min and a flotation tank volume of 40 mL. 2 g of ore sample and 32 mL of deionized water were added for each experiment, and the process was carried out in the order of stirring, adjusting the pH value of the slurry, inhibitor action, collector action, and flotation recovery for 2 minutes.

The XFG-Ⅱ hanging-trough flotation machine manufactured by Jilin Prospecting Machinery Factory was used in the microflotation test (Gong et al., 2023c). In the flotation-test, a 2.0-g mineral sample was placed in a 40-mL flotation tank, and 32-mL deionized water was added. The procedure followed a sequence of stirring, slurry conditioning, depressant addition, collector addition, and flotation, with each step lasting approximately 2 minutes (Gong et al, 2024a). In this study, the selectivity index (SI) was used to evaluate the separation efficacy of the diaspore–kaolinite system when the GG was used. The selectivity index was calculated using Eq. (1) (Yang et al., 2025):

$$SI = \sqrt{\frac{R_d \times J_k}{(1000 - R_d) \times (100 - J_k)}} \quad (1)$$

where SI represents the selectivity index, and R_d and J_k represent the recoveries of diaspore in the concentrate and kaolinite in the tailing, respectively.

The static contact-angle of deionized water on the mineral surface was measured using the hanging-drop method in a JC2000A contact-angle measuring instrument (Gong et al., 2024b). The sample for the contact-angle measurement was prepared according to a singlemineral flotation-test procedure. After the sample was filtered and naturally air dried, the powder sample was pressed into a cylindrical, dense, and smooth sheet. The sheet was placed on a measuring platform, a drop of liquid was introduced using a microsyringe, and the wetting picture of the mineral surface liquid was collected to obtain the mineral surface contact-angle.

The zeta-potential measurement was performed in a NanoZS90-2000-type potential analyzer manufactured by Malvern Instruments Limited in the UK (Han et al., 2026). Before the measurement, the ore sample was ground to smaller than 5 μm. At each measurement, 30 mg of the sample was put into a 50-mL beaker, and a 50-mL KCl solution (1×10^{-3} mol/L) was added as an electrolyte solution. The slurry was then stirred for 2 min using a magnetic stirrer for full dispersion. We adjusted the pulp pH using HCl or NaOH solution and added a flotation reagent as needed, stirring it for 3 min. After the slurry was made to stand for 10 min, 1 mL of upper suspension was taken for testing, and the galvanic potential value of each group was measured three times to calculate the average value.

The Nicolet 380 infrared spectrum analyzer produced by Thermo Fisher Technology Co., Ltd. (United States) was used to measure the infrared spectra (Wen et al., 2025). For this, the two mineral samples were ground < 5 μm. The pure mineral samples of diaspore and kaolinite were fully treated with flotation reagents according to the flotation test process, and the treated samples were repeatedly cleaned three times and naturally air dried. Further, the samples treated with or without flotation reagents were mixed with KBr at a mass ratio of 1:100, and the infrared spectra of the samples were measured after pressing.

XPS spectra of diaspore and kaolinite before and after flotation reagents were measured using an ESCALAB 250 spectrograph (Thermo Scientific K-Alpha) (Yu et al., 2025). The test samples were prepared following the flotation test process, cleaned with deionized water and air-dried at room temperature before being sent for testing. To calibrate all binding energies, a neutral C 1s carbon peak (284.80 eV) was employed, and Thermo Avantage software was used to process the measurement.

3. Results and discussions

3.1. Micro-flotation test results

Initially, micro-flotation experiments were conducted at a pulp pH of 10 to evaluate how collector dosage affects the flotation recovery of diaspore and kaolinite. The relationship between SDS concentration and the recovery of these minerals is presented in Fig. 3.

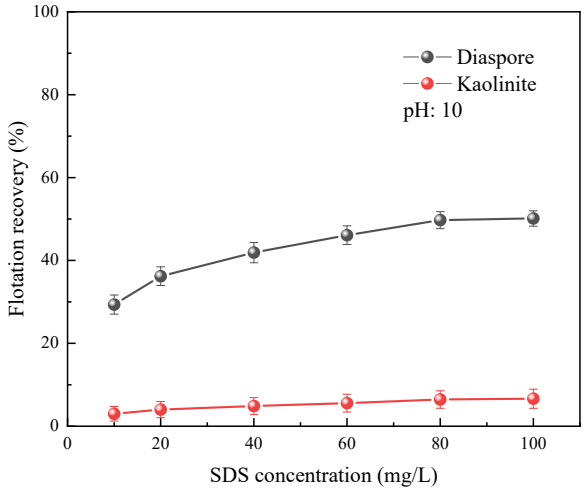


Fig. 3. Effect of SDS concentration on flotation recovery of diaspore and kaolinite

According to Fig. 3, the recovery of diaspore remains below 50%, while that of kaolinite is less than 7%, indicating that neither mineral exhibits satisfactory floatability under this pH condition. At this specific concentration (80 mg/L), the maximum flotation recovery difference between the two minerals reaches 43.3%. Consequently, using this SDS concentration, further experiments were designed to examine the effect of pulp pH on the flotation recovery of the two minerals.

Fig. 4 shows that at a pulp pH of 2, the maximum recoveries of diaspore and kaolinite reach 97.17% and 36.36%, respectively. Under this condition, the flotation recovery difference between the two minerals peaks at 60.81%. Given the high recovery of diaspore and the relatively small flotation contrast between the two minerals at pH 2, further experiments were conducted to evaluate how guar gum affects their flotation recovery under the same pH condition.

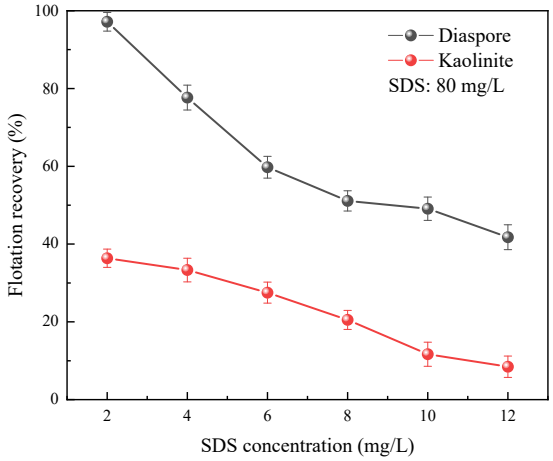


Fig. 4. Effect of pH value on floatability of diaspore and kaolinite

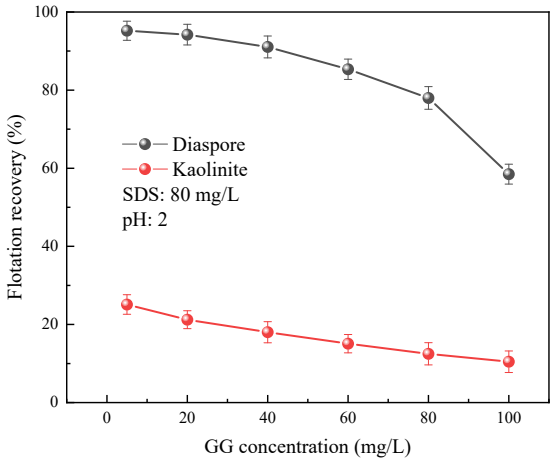


Fig. 5. Effect of GG Concentration on flotation recovery of diaspore and kaolinite

Fig. 5 shows that the decline range of diaspore gradually increases, while that of kaolinite decreases. At a GG concentration of 20 mg/L, the maximum flotation difference between the two minerals reaches 72.99%, representing the most favorable condition for their separation. Accordingly, the separation performance of an artificial diaspore-kaolinite mixture was investigated at pH 2, with SDS at 80 mg/L and GG at 20 mg/L.

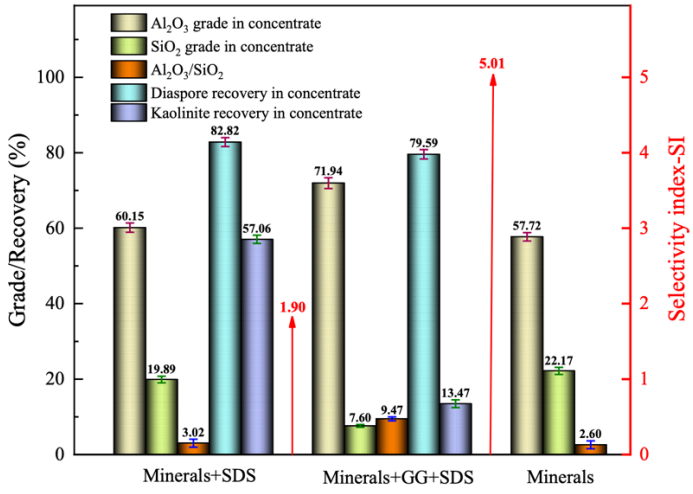


Fig. 6. Effect of GG on flotation separation of kaolinite from diaspore

Fig. 6 shows that the original mixed ore of diaspore and kaolinite has an Al_2O_3 grade of 57.72%, SiO_2 grade of 22.17%, and an Al_2O_3/SiO_2 ratio (A/S) of 2.60. Treatment with SDS alone yields a concentrate with 60.15% Al_2O_3 (up 2.43%), 19.89% SiO_2 (down 2.28%), and an A/S of 3.02. The recoveries of diaspore and kaolinite in the concentrate are 82.82% and 57.06%, respectively, with a selective separation index of 1.90. These results indicate poor separation of the two minerals using SDS alone.

In contrast, under the combined action of GG and SDS, the concentrate achieves an Al_2O_3 grade of 71.94% (up 14.22%), a SiO_2 grade of 7.60% (down 14.57%), and an A/S of 9.47. The recoveries of diaspore and kaolinite are 79.59% and 13.47%, respectively, with a selectivity index of 5.01. These findings demonstrate that GG inhibits kaolinite flotation, reduces SiO_2 content in the concentrate, raises the A/S ratio, and thereby enables effective separation of diaspore from kaolinite.

3.2. Contact angle analysis

Micro-flotation tests show that GG slightly affects diaspore recovery but significantly inhibits kaolinite flotation. Since reagent separation performance is closely tied to surface hydrophobicity (Gong et al., 2025), contact angles of both minerals were measured before and after reagent treatment, with results shown in Fig. 7.

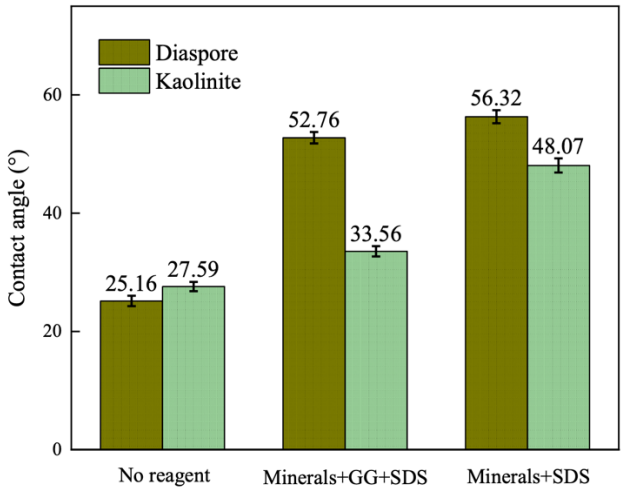


Fig. 7. Contact angle of diaspore and kaolinite before and after flotation reagent action

In deionized water, the contact angles of diaspore and kaolinite are 25.16° and 27.59°, respectively, indicating poor natural floatability. With SDS alone, the contact angle of diaspore rises to 56.32° (an increase of 31.16°), and that of kaolinite to 48.07° (up by 20.48°), suggesting significantly enhanced surface hydrophobicity for both. Under combined GG and SDS treatment, the contact angles become 52.76° for diaspore and 33.56° for kaolinite, decreasing by 3.56° and 14.51°, respectively. This indicates that kaolinite becomes less hydrophobic while diaspore retains its hydrophobicity. Consequently, a marked difference in floatability emerges between the two minerals: diaspore remains readily floatable, whereas kaolinite loses much of its floatability.

3.3. Zeta potential analysis

Reagent adsorption on mineral surfaces alters zeta potential, thereby affecting floatability (Chen and Zhang, 2025). To understand how GG influences the surface electrical properties of diaspore and kaolinite, zeta potential was measured before and after GG interaction, with results shown in Fig. 8.

As pH increases from 2 to 12, the negative charge on both minerals gradually rises. The isoelectric points (IEPs) of diaspore and kaolinite are approximately 5.33 and 4.62, respectively. After GG treatment, the IEP of diaspore shifts to 4.71 (a change of 0.62), while that of kaolinite shifts to 2.54 (a change of 2.08). This indicates weak adsorption of GG on diaspore but strong adsorption on kaolinite.

Under flotation conditions at pH 2, the zeta potentials of diaaspore and kaolinite are 17.82 mV and 14.94 mV, respectively. Following GG addition, these values drop to 13.18 mV and 3.24 mV, corresponding to shifts of 4.64 mV and 11.7 mV. The smaller shift for diaspore and larger shift for

kaolinite further confirms that GG adsorbs weakly on diaspore but strongly on kaolinite, thereby exerting a strong inhibitory effect on kaolinite flotation.

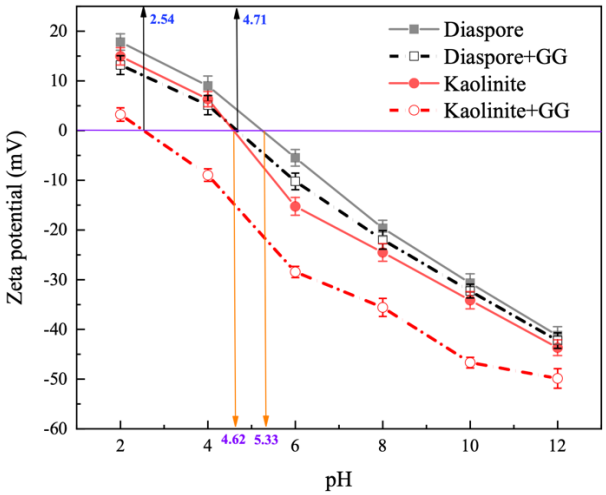


Fig. 8. Zeta potential of diaspore and kaolinite before and after GG treatment

3.4. FTIR analysis

Zeta potential analysis revealed how GG adsorbs onto diaspore and kaolinite surfaces, but did not address the effect of GG on SDS adsorption (Gong et al., 2023). To explore this under coexisting conditions, infrared spectroscopy was performed, with results shown in Figs. 9–11.

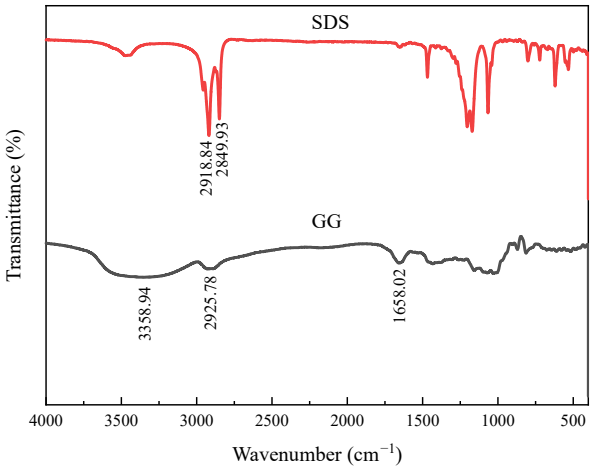


Fig. 9. Infrared spectra of SDS and GG

In Fig. 9, SDS exhibits prominent characteristic peaks at 2918.84 cm^{-1} and 2849.93 cm^{-1}, corresponding to the antisymmetric stretching vibrations of methyl ($-CH_3$) and methylene ($-CH_2$), respectively (Wei et al., 2021; Gong et al., 2023d). For GG, its hydroxyl (–OH) stretching vibration peak appeared at 3358.94 cm^{-1}, characteristic peaks appear at 2925.78 cm^{-1} and 1658.02 cm^{-1}, attributed to the antisymmetric stretching vibration of methylene ($-CH_2$) and the tensile vibration of the carboxane six-membered ring, respectively (Gong et al., 2023a; Tan et al., 2020). Fig. 10 shows that diaspore has characteristic peaks at 746.24, 959.82, 1984.56, and 3113.77 cm^{-1}. With SDS alone, peaks at 2849.93 and 2918.92 cm^{-1} (attributable to SDS) appear on the diaspore surface, indicating SDS adsorption. When GG and SDS are combined, SDS-related peaks still appear at 2849.71 and 2919.05 cm^{-1}, confirming that SDS can still adsorb onto diaspore in the presence of GG.

As shown in Fig. 11, kaolinite exhibits characteristic peaks at 692.88, 913.22, 3618.65, and 3692.36 cm^{-1}. After SDS treatment alone, peaks at 2851.61 and 2919.54 cm^{-1} appear, indicating SDS adsorption on kaolinite. However, after combined GG and SDS treatment, these SDS peaks disappear, demonstrating that GG hinders SDS adsorption on kaolinite.

Thus, GG hardly affects SDS adsorption on diaspore but inhibits it on kaolinite, favoring selective collection of diaspore by SDS and promoting flotation separation of the two minerals.

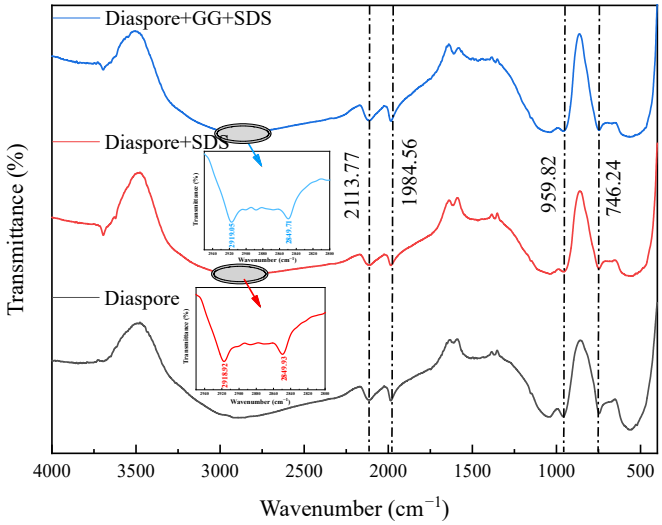


Fig. 10 Effect of flotation reagent on infrared spectra of diaspore

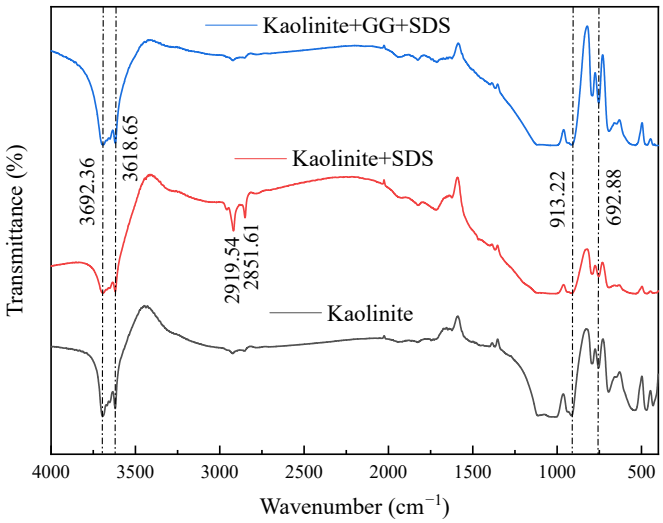


Fig. 11. Effect of flotation reagent on infrared spectra of kaolinite

3.5. XPS analysis

Zeta potential and infrared spectroscopy revealed the adsorption behavior of the inhibitor GG on diaspore and kaolinite, along with its influence on SDS collector adsorption. However, the underlying reasons for GG's selective adsorption remain unclear. To address this, XPS analysis was employed to identify the adsorption sites of GG on the two mineral surfaces, further clarifying its selective adsorption mechanism (Rezvani et al., 2025; Fan and Xu, 2026).

As shown in Fig. 12, the SDS spectrum displays three major peaks: C 1s, O 1s, and S 2p, with S 2p serving as its characteristic peak. The GG spectrum exhibits four major peaks: C 1s, O 1s, N 1s, and P 2p, where N 1s and P 2p are its characteristic peaks.

As shown in Fig. 13, the diaspore surface displays four distinct peaks: Al 2p, Al 2s, C 1s, and O 1s. After SDS treatment alone, an S 2p peak appears, indicating SDS adsorption on diaspore. After GG treatment alone, a N 1s peak emerges, suggesting GG adsorption. However, under combined SDS and GG treatment, only the S 2p peak appears, demonstrating that GG adsorbs weakly on diaspore, while SDS adsorbs strongly.

In contrast, Fig. 14 shows six distinct peaks on the kaolinite surface: Al 2p, Al 2s, Si 2p, Si 2s, C 1s, and O 1s. After SDS only, an S 2p peak appears, indicating SDS adsorption on kaolinite. After GG only,

a N 1s peak appears, indicating GG adsorption. Under combined treatment, only a pronounced N 1s peak is observed, revealing that GG adsorbs strongly on kaolinite, whereas SDS adsorbs weakly.

In summary, while SDS alone can adsorb onto both minerals, GG selectively and strongly adsorbs onto kaolinite. In the presence of GG, SDS adsorbs strongly on diaspore but weakly on kaolinite, explaining why diaspore floats while kaolinite sinks during flotation.

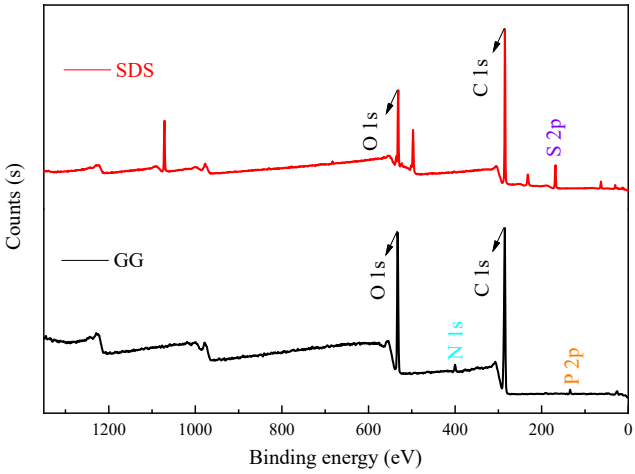


Fig. 12 XPS full spectrum of SDS and GG

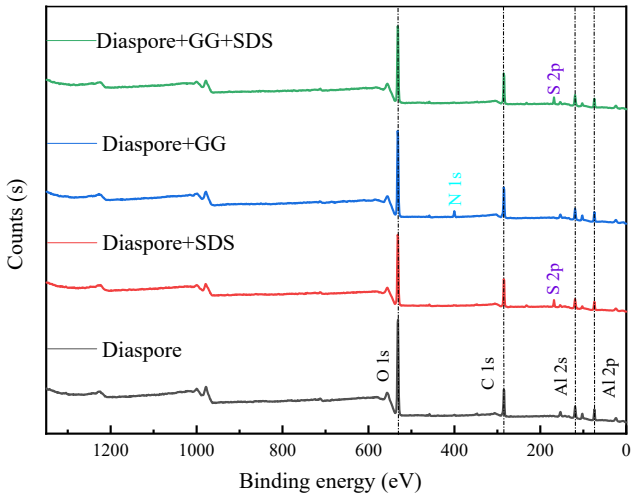


Fig. 13 Full XPS spectra of diaspore surface before and after SDS and GG

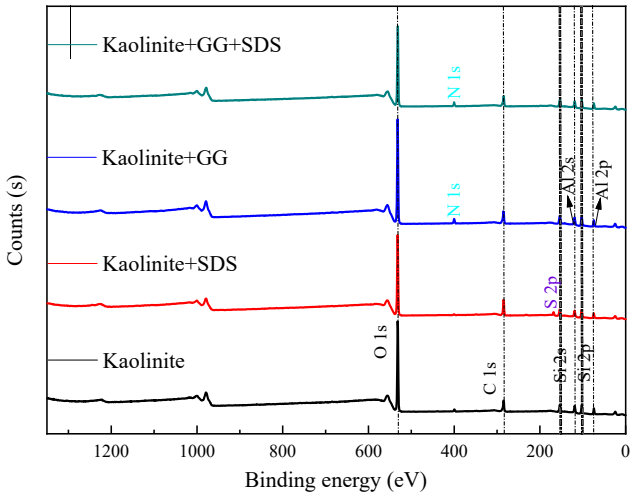


Fig. 14. Full XPS spectra of kaolinite surface before and after SDS and GG

To further determine the adsorption sites and strengths of GG on mineral surfaces, fine XPS spectra of Al sites on diaspore and Al/Si sites on kaolinite were analyzed before and after GG interaction, with results shown in Figs. 15−17.

As shown in Fig. 15, the Al 2p peaks of diaspore appear at 74.18 eV and 74.69 eV. After GG treatment, these shift slightly to 74.21 eV and 74.72 eV, a change of only 0.03 eV. Such a minor shift (less than 0.2 eV) indicates weak GG adsorption on the Al sites of diaspore (Xie et al., 2022).

Fig. 16 shows that the Al 2p peaks of kaolinite are at 74.09 eV and 74.63 eV. After GG treatment, they shift to 74.15 eV and 74.69 eV, a change of 0.06 eV. Again, the shift remains below 0.2 eV (Budemberg et al., 2025), suggesting weak GG adsorption on Al sites of kaolinite as well.

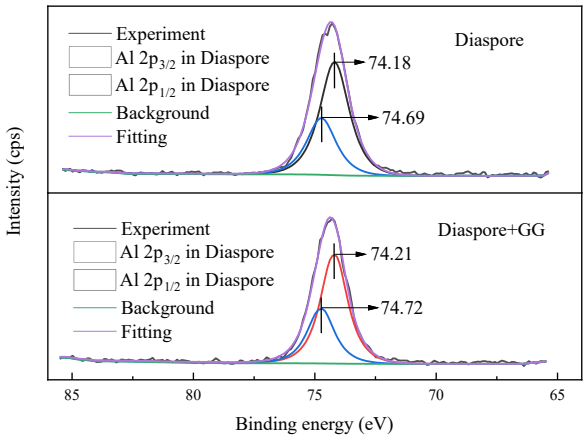


Fig. 15. Fine spectra of Al site in diaspore before and after GG

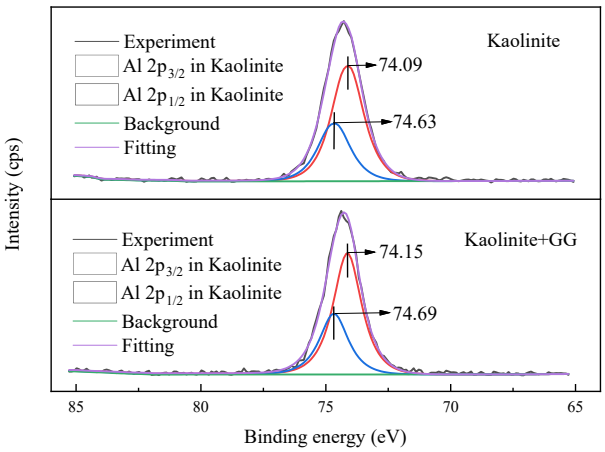


Fig. 16. Fine spectra of Al site in kaolinite before and after GG

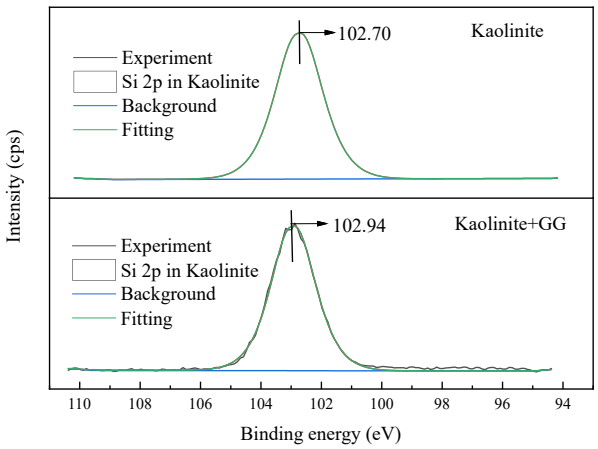


Fig. 17. Fine spectra of Si site in kaolinite before and after GG

In contrast, Fig. 17 reveals that the Si 2p peak of kaolinite shifts from 102.70 eV to 102.94 eV after GG treatment, a change of 0.24 eV. This significant shift indicates strong GG adsorption on the Si sites of kaolinite.

To further explain the selectivity of GG adsorption on kaolinite, the relative surface concentrations of major elements before and after GG treatment were analyzed (Fig. 18).

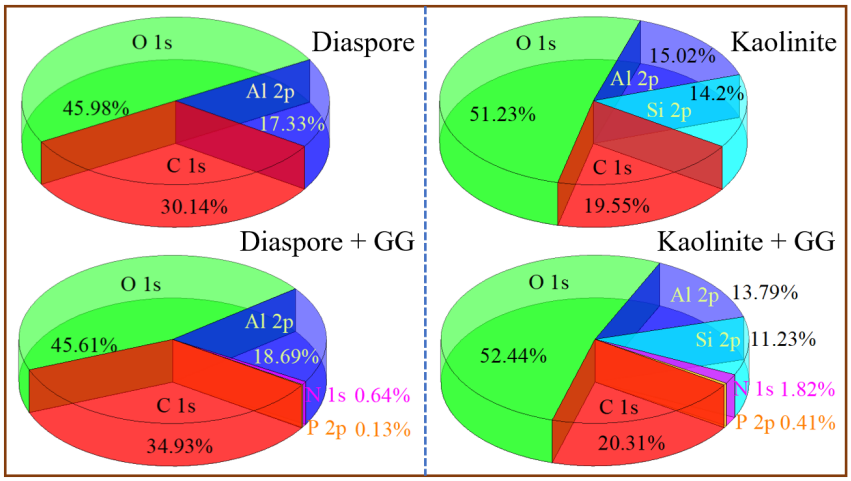


Fig. 18. Effect of GG on surface elemental composition of diaspore and kaolinite

The relative content of Al on diaspore changes from 17.33% to 18.69% after GG treatment (a 1.36% change), while on kaolinite it changes from 15.02% to 13.79% (a 1.23% change). These similar variations confirm that GG affects the Al sites of both minerals comparably. However, the Si content on kaolinite drops from 14.20% to 11.23% after GG treatment (a 2.97% change), a much more pronounced shift, further confirming that GG adsorbs strongly onto Si sites (Zhang et al., 2026; Yu et al., 2024).

Moreover, the characteristic N and P contents of GG on kaolinite (1.82% and 0.41%, respectively) are approximately three times higher than those on diaspore (0.64% and 0.13%), indicating far stronger adsorption of GG on kaolinite.

In summary, GG exhibits strong adsorption on the Si sites of kaolinite but weak adsorption on the Al sites of both minerals. During flotation, GG selectively adsorbs onto kaolinite, blocking SDS adsorption on its surface, thereby inhibiting kaolinite flotation and enabling its separation from floating diaspore.

3.6. Discussion

3.6.1. The charge characteristics of GG in solution

The types of atoms in the molecular formula of guar bean gum (GG) can infer its potential functional groups containing phosphorus groups. The P and O atoms in the molecular formula indicate the presence of phosphate or phosphonic acid groups. The phosphate group is a typical anionic functional group, with pKa values typically around 2, 7, and 12 (the first step dissociation $pKa_1 \approx 2.1$ for phosphate, the second step $pKa_2 \approx 7.2$, and the third step $pKa_3 \approx 12.3$), at pH=2, the dissociation of the second and third steps can be ignored. According to the Henderson Hasselbach equation, the dissociation degree is calculated. At pH 2, the phosphate groups partially dissociate, with each phosphate group carrying an average negative charge of approximately -0.44. However, due to the low concentration of phosphate groups, these groups were not detected in infrared spectroscopy analysis.

3.6.2. Floatation advantage at pH 2

The advantages of flotation at pH 2 are mainly reflected in high selectivity and collection performance. At pH 2, the surface of kaolinite is mainly dominated by protonated silanol groups ($\equiv Si\text{-}OH_2^+$), which facilitate hydrogen bonding with guar gum, while the reactivity of the surface of monohydrate alumina ($\equiv Al\text{–}OH$) to GG is relatively low. Therefore, this pH condition maximizes the selectivity of GG inhibitors.

3.6.3. Comparative analysis of collector SDS and NaOl

There are two main considerations when choosing sodium dodecyl sulfonate (SDS) as a collector. One is to consider pH compatibility. At pH 2, sodium oleate (NaOl) undergoes protonation to form oleic acid (with a pKa of approximately 4.8-5.0), which significantly reduces its solubility and surface activity. In contrast, the pKa of the sulfonic acid head group of SDS is much lower (about 1-2), so SDS can still fully ionize and maintain surface activity at pH 2. Secondly, consider selectivity. The sulfonic acid group of SDS can have a stronger affinity for the Al–OH sites on the surface of diaspore through specific interactions, while the carboxylic acid group of NaOl often non selectively adsorbs on the Al–OH and Si–OH sites under acidic conditions.

3.6.4. Floatation disadvantage at pH 2

The disadvantages of flotation at pH 2 include equipment corrosion and wastewater treatment. Operating at pH 2 requires the use of acid resistant materials for flotation cells, pipelines, and pumps, which increases capital and maintenance costs in industrial applications. In addition, acidic tailings water needs to be neutralized before discharge, which will increase the environmental and operational burden.

Overall, for this specific mineral system, the significant improvement in separation selectivity at pH 2 exceeds the operational disadvantages.

3.6.5. Strong adsorption on Si sites

The siloxane base of kaolinite does not possess high-density silanol (≡Si–OH) groups. Its inertness comes from the participation of lone pair electrons of Si-O-Si bridging oxygen to form π bonds, with weak hydrogen bond acceptance ability and a lack of hydrogen bond donors. Si sites are more conducive to the adsorption of guar gum, which is closely related to the barrier effect of the surface hydration layer. There is usually a thick and stable hydration layer on the surface of aluminum oxides such as diaspore, which acts as a barrier to prevent guar gum from approaching the surface Al–OH sites. In contrast, the hydration layer on the surface of kaolinite is discontinuous, making it easier for guar gum to come into contact with and adsorb onto silanol/alkyl groups. In addition, XPS analysis showed a significant chemical shift in the Si 2p peak after adsorption with guar gum, while the Al 2p peak remained largely unchanged. This further supports the conclusion that Si sites have specific chemical contributions while Al sites lack such effects.

4. Conclusion

1. GG has achieved flotation separation of diaspore and kaolinite, with an Al/Si ratio of 9.47.
2. GG significantly reduces the contact angle of kaolinite and strongly adsorbs on its surface.
3. GG hinders the collection of kaolinite by SDS, but does not affect the collection of diaspore by SDS.
4. GG is selectively adsorbed on Si sites on kaolinite surface, but the adsorption ability on Al sites of the two minerals is weak.

Acknowledgments

This work was financially supported by the National Natural Science Foundation of China (Grant No. 52474288). Special thanks are due to the instrumental or data analysis from Analytical and Testing Center, Northeastern University.

References

BICAK O., EKMEKCI Z., BRADSHAW D.J., HARRIS P.J., 2007, *Adsorption of guar gum and CMC on pyrite*, Minerals Engineering, 20(10), 996-1002.

BUDEMBERG G., JOLSTERÅ R., CHELGANI S.C., 2025, *Eco-friendly collectors in apatite froth flotation: A review*, International Journal of Mining Science and Technology, 35(4), 539-551.

CHANG Z., SUN C., KOU J., FU G., QI X., 2021, *Experimental and molecular dynamics simulation study on the effect of polyacrylamide on bauxite flotation*, Minerals Engineering, 164.

CHEN J.H., ZHANG Y.B., 2025, *Large system study of chalcopyrite and pyrite flotation surfaces based on SCC-DFTB parameterization method*, International Journal of Mining Science and Technology, 35(7), 1037-1055.

DING Y., FENG S., XIA X., TIAN Y., WU C., DUAN G., 2026, *Process optimization for preparation of anhydrite- Ⅱ via lime neutralization coupled with medium-temperature calcination*, China Powder Science and Technology, 32(2), 216-226.

FAN F., XU Y., 2026, *Microkinetic model and numerical simulations of particulate acoustic agglomeration*, China Powder Science and Technology, 32(1), 33-43.

GONG X., YAO J., GUO J., YANG B., SUN H., YIN W., WANG Y., FU Y., 2024b, *Role of tannin pretreatment in flotation separation of magnesite and dolomite*, International Journal of Minerals Metallurgy and Materials, 31(3), 452-461.

GONG X., YAO J., YANG B., FU Y., WANG Y., YIN W., 2023c, *Selective flotation of brucite from calcite using HEDP-4Na as an inhibitor in a SDS system*, Journal of Industrial and Engineering Chemistry, 125, 390-401.

GONG X., YAO J., YANG B., GUO J., SUN H., YIN W., 2023a, *Study on the inhibition mechanism of guar gum in the flotation separation of brucite and dolomite in the presence of SDS*, Journal of Molecular Liquids, 380.

GONG X., YAO J., YANG B., YIN W., GUO J., SONG N., WANG Y., SUN H., 2023b, *Activation-inhibition mechanism of diammonium hydrogen phosphate in flotation separation of brucite and calcite*, Journal of Environmental Chemical Engineering, 11(3).

GONG X., YAO J., YANG B., YIN W., WANG Y., FU Y., 2023, *Selective adsorption of the activator diammonium hydrogen phosphate in the reverse flotation separation of brucite and dolomite*, Powder Technology, 429.

GONG X., YAO J., YANG B., YIN W., WANG Y., FU Y., 2024a, *Flotation separation of brucite and calcite in dodecylamine system enhanced by regulator potassium dihydrogen phosphate*, Transactions of Nonferrous Metals Society of China, 34(8), 2658-2670.

GONG X., YAO J., YANG B., ZHU Z., GUO J., YIN W., FU Y., WANG Y., 2023d, *An environment-friendly and highly effective inhibitor for flotation separation of brucite and dolomite in SDS system*, Separation Science and Technology, 58(10), 1784-1794.

GONG X., YAO J., YIN W., SONG N., WANG Y., 2024a, *Effect of Surface Dissolution on the Floatability of Brucite in Three Anionic Collector Systems*, Surface and Interface Analysis.

GONG X.F., YAO J., JIA Y.K., YIN C., YIN W.Z., WANG Y.L., FU Y.F., 2025, *Surface pretreatment effect on the separation and purification of magnesite and dolomite*, Journal of Central South University, 32(3), 977-990.

HAN H., XIE K., ZHAO Y., WANG Y., SUN H., ZHANG Z., YUAN Z., 2026, *Influence of different dispersants on dispersion characteristics of carbonate-containing mixed magnetic concentrates*, China Powder Science and Technology, 32(2), 89-100.

HASSAN A., RUDOLPH M., VINNETT L., ECKERT K., PEREIRA L., 2025, *An approach to quantify the true flotation recovery of floatable minerals using natural entrainment tracers and particle-based separation modeling*, International Journal of Mining Science and Technology, 35(8), 1233-1244.

JIANG H., SUN Z., XU L., HU Y., HUANG K., ZHU S., 2014, *A comparison study of the flotation and adsorption behaviors of diaspore and kaolinite with quaternary ammonium collectors*, Minerals Engineering, 65, 124-129.

LI H., CHAI W., CAO Y., WU Y., YANG S., 2021, *Synergistic collection mechanism of D-phenylalanine and sodium oleate in flotation of diaspore from kaolinite*, Applied Surface Science, 538.

LIU C., HU Y., FENG A., GUO Z., CAO X., 2011, *The behavior of N,N-dipropyl dodecyl amine as a collector in the flotation of kaolinite and diaspore*, Minerals Engineering, 24(8), 737-740.

OUYANG L., WU J., HUANG Z., BURDONOV A.E., VCHISLO N.V., WANG H., HE G., YU X., MA J., LI W., 2024, *A novel 3-tetradecylamine propyl amidoxime collector for highly efficient flotation of fine kaolinite*, Powder Technology, 445.

RATH R.K., SUBRAMANIAN S., PRADEEP T., 2000, *Surface chemical studies on pyrite in the presence of polysaccharide-based flotation depressants*, Journal of Colloid and Interface Science, 229(1), 82-91.

REZVANI A., RAJI F., FAN R., KAPPES R., GAO Z.Y., PENG Y.J., 2025, *Depression of pyrrhotite superstructures in copper flotation: A synchrotron X-ray powder diffraction and DFT study*, International Journal of Mining Science and Technology, 35(8), 1259-1270.

SZERENYI D., STOLK P., TOVARI J., TAKACS L., GUTTMAN A., 2025, *Development of a High-Performance Immunoaffinity Separation Technique for Rare Cell Capture*, Separations, 12(5).

TAN X., ZHU Y., SUN C., ZHANG X., SU J., 2020, *Adding cationic guar gum after collector: A novel investigation in flotation separation of galena from sphalerite*, Minerals Engineering, 157.

VIDAL C.A.G., PAWLIK M., 2015, *Molecular weight effects in interactions of guar gum with talc*, International Journal of Mineral Processing, 138, 38-43.

WANG J., SOMASUNDARAN P., NAGARAJ D.R., 2005, *Adsorption mechanism of guar gum at solid-liquid interfaces*, Minerals Engineering, 18(1), 77-81.

WEI Z., SUN W., HAN H., LIU G., FU J., XING Y., 2021, *Probing a colloidal lead-group multiple ligand collector and its adsorption on a mineral surface*, Minerals Engineering, 160.

WEN S.M., MIAO Y.C., TANG Y.Y., SONG Z.Y., FENG Q.C., 2025, *Theoretical and experimental study on high-entropy flotation of micro-fine cassiterite*, International Journal of Mining Science and Technology, 35(1), 19-39.

XIA L., ZHONG H., LIU G., WANG S., 2009, *Utilization of soluble starch as a depressant for the reverse flotation of diaspore from kaolinite*, Minerals Engineering, 22(6), 560-565.

XIE R., TONG X., XIE X., ZHU Y., LIU J., 2022, *Flaxseed gum as new depressant in the separation of apatite and dolomite and its mechanism*, Applied Surface Science, 593.

XIE Y., YIN W.Z., LIU Q., WANG D.W., SUN W.J., 2025, *Reverse floc-flotation of talc from chalcopyrite by using polyvinyl acetate as a flocculant: Adsorption and bubble capture studies*, International Journal of Mining Science and Technology, 35(10), 1775-1788.

XU J., HU S., 2026, *Research progress on adsorption and separation of fluorohydrocarbons by porous materials*, China Powder Science and Technology, 32(1), 1-13.

YANG B., HE J., 2025, *New insights into selective depression mechanism of Tamarindus indica kernel gum in flotation separation of fluorapatite and calcite*, Separation and Purification Technology, 354.

YANG B., LI J., HE J.F., ZHU L.T., GUO S.H., ZHANG S., 2025, *Differentiated regulation of mineral interface properties using an eco-friendly polysaccharide depressant for enhanced apatite-dolomite sustainable flotation separation*, Green Chemistry, 27(47), 15211-15224.

YU J., GONG X., YAO J., YIN W., XUE F., TIAN D., WANG Y., 2024, *Analysis of flotation separation mechanism of magnesite and calcite and their interaction with bubbles*, Powder Technology, 446.

YU J., YAO J., GONG X., YIN X., YIN W., CAO Y., 2025, *Effect of polycarboxylate superplasticizer on flotation separation of*, *limonite and calcite. Journal of Molecular Liquids, 438.

YU J.W., YAO J., YIN W.Z., GONG X.F., DU W.F., ZHAO X., 2025, *Theoretical study on the flotation and adsorption behavior of dodecylamine on hydroxide minerals*, Particulate Science and Technology, 43(8), 1384-1397.

YU J.W., YAO J., YIN W.Z., GONG X.F., YIN X.M., ZHAO X., 2025, *Study on the adsorption mechanism of green and efficient flotation reagents in the reverse flotation separation of limonite and quartz*, Colloids and Surfaces a-Physicochemical and Engineering Aspects, 726.

YU Y., WANG Y., ZHU Y., ET AL., 2024, *Optimization of nesquehonite whisker preparation process based on BP neural network*, China Powder Science and Technology, 30(1), 103-113.

ZHANG N., EJTEMAEI M., NGUYEN A.V., ZHOU C., 2019, *XPS analysis of the surface chemistry of sulfuric acid-treated kaolinite and diaspore minerals with flotation reagents*, Minerals Engineering, 136, 1-7.

ZHANG S., REN J., WEN Y., SHAO X., 2022, *Flotation separation of diaspore and kaolinite by using dodecanamide and cetyltrimethylammonium bromide as an effective mixed collector*, Minerals Engineering, 179.

ZHANG Y., LI S., SONG Z., YANG Y., BAI L., YU X., ZHAO， L., MA J., 2026, *Research progress on selective flocculation–flotation of fine-grained minerals*, Green and Smart Mining Engineering, 3, 180-193.

ZHAO N., ZHANG Q., MA H.W., SUN Y.S., GAO P., CAO Z., ZHANG Z.Y., 2025, *Advancing the recovery of iron and rare earth elements from the solid waste at Bayan Obo*, International Journal of Mining Science and Technology, 35(2), 295-306.